

Automatically Generating UI Code from Screenshot: A Divide-and-Conquer-Based Approach

Yuxuan Wan

The Chinese University of Hong Kong
Hong Kong, China
yxwan9@cse.cuhk.edu.hk

Chaozheng Wang

The Chinese University of Hong Kong
Hong Kong, China
czwang23@cse.cuhk.edu.hk

Yi Dong

The Chinese University of Hong Kong
Hong Kong, China
1155173962@link.cuhk.edu.hk

Wenxuan Wang

The Chinese University of Hong Kong
Hong Kong, China
wxwang@cse.cuhk.edu.hk

Shuqing Li

The Chinese University of Hong Kong
Hong Kong, China
sqli21@cse.cuhk.edu.hk

Yintong Huo*

The Chinese University of Hong Kong
Hong Kong, China
ythuo@cse.cuhk.edu.hk

Michael R. Lyu

The Chinese University of Hong Kong
Hong Kong, China
lyu@cse.cuhk.edu.hk

ABSTRACT

Websites are critical in today’s digital world, with over 1.11 billion currently active and approximately 252,000 new sites launched daily. Converting website layout design into functional UI code is a time-consuming yet indispensable step of website development. Manual methods of converting visual designs into functional code present significant challenges, especially for non-experts. To explore automatic design-to-code solutions, we first conduct a motivating study on GPT-4o and identify three types of issues in generating UI code: element omission, element distortion, and element misarrangement. We further reveal that a focus on smaller visual segments can help multimodal large language models (LLMs) mitigate these failures in the generation process.

In this paper, we propose DCGen, a divide-and-conquer-based approach to automate the translation of webpage design to UI code. DCGen starts by dividing screenshots into manageable segments, generating descriptions for each segment, and then reassembling them into complete UI code for the entire screenshot. We conduct extensive testing with a dataset comprised of real-world websites and various LLMs and demonstrate that DCGen achieves up to a 14% improvement in visual similarity over competing methods. To the best of our knowledge, DCGen is the first segment-aware prompt-based approach for generating UI code directly from screenshots.

1 INTRODUCTION

Websites are important in today’s digital landscape, serving as essential platforms for diverse applications in our daily lives. Statistics show that there are over 1.1 billion online websites, with approximately 252,000 new websites being created every day [1, 3].

Developing a website’s graphical user interface (GUI) involves two successive activities: designing and implementing the user interface (UI). UI design contains graphic artists designing and customizing the website layout, which is then conveyed to developers

in pixel-based concept drawings [13, 38]. Afterward, UI implementation focuses on converting the visual design into functional UI code using GUI frameworks.

Manually implementing visual designs of websites into functional code is complicated and time-consuming, as it requires domain knowledge of mapping GUI framework elements to spatial layouts. For laypersons, this knowledge barrier has hindered them from efficiently building their own web applications, even if they have concrete ideas for the design [62]. For developers, acquiring such knowledge is challenging, time-consuming, and error-prone due to the intricate nature of GUI frameworks, marked by the excessive amount of GUI components, the complexity of spatial layouts, and the diversity of GUI frameworks [13, 40, 50, 52]. Although modern GUI builders provide interactive features (e.g., drag & drop, what-you-see-is-what-you-get) for developing a GUI, these tools often limit customization [52], causing discrepancies between the intended design and actual implementation, and are known to introduce bugs and presentation failures even for simple tasks [76].

The challenges in GUI production necessitate an automated approach to translating UI designs (e.g., images, sketches) into GUI code, referred to as *Design-to-Code*. The automated design-to-code techniques offer benefits to individuals and companies. First, it has the potential to democratize front-end web application development [52], allowing non-experts to easily build web applications. Second, it allows smaller companies to focus more on visual features, rather than on translating designs into functional code [49].

Despite its promising benefits, practical solutions for generating code implementation from website design have been underexplored. A line of research made efforts to transform GUI design into code for Android mobile apps but these approaches are not generalizable to the website design containing complicated interfaces [5, 13, 49, 52]. To enable finger-friendly touch targets, mobile apps utilize minimalist designs to avoid clutter on small screens, resulting in fewer visual elements and simpler structures. Additionally, mobile development relies on platform-specific tools [36] (e.g., iOS uses Xcode, Android uses Android Studio), which do not apply to website development that typically uses HTML, CSS, and JavaScript [2, 4, 61]. Another

*Yintong Huo is the corresponding author.

line of research generates website UI code from screenshots using deep learning-based techniques (e.g., CNN, LSTM), but they rely on synthetic data. For example, Beltramelli et al. [11] integrates CNN and RNN models to generate code from screenshots. However, this method is limited to a narrow range of simple user interface designs, accommodating only five types of web elements. Despite training on pairs of screenshots and code, DL-based approaches are still restricted by their training data which may contain limited web elements and programming knowledge. In a nutshell, existing studies are unsuitable for building real-world software websites.

Multimodal Large Language Models (MLLMs) have seen significant advancements recently [23, 32, 54], offering an alternative solution for design-to-code. By integrating image processing capabilities into large language models (LLMs), MLLMs have demonstrated superior ability than CNNs for understanding images and answering visual questions [72]. Furthermore, research has shown that LLMs have remarkable performance on various code intelligence tasks [35], including code generation [26, 28, 31, 37, 42, 75], code completion [16, 24, 25, 43, 44, 53], and code summarization [9, 14, 30, 34, 46, 47]. The strong image understanding and code generation capabilities of MLLMs showcase their potential to transform website screenshots into functional web code.

Unfortunately, notwithstanding MLLMs’ impressive performance in image-to-text tasks, directly applying them for UI code generation results in unsatisfactory performance because of the complicated nature of GUI. Unlike generating general descriptions, translating images into UI code poses unique challenges for MLLMs. Firstly, it must accurately detect and classify diverse elements and nested structures within a single webpage, such as buttons, text fields, and images. Secondly, it demands the precise replication of intricate layouts and styles. Modern GUIs cannot be constructed merely through the hardcoded positioning of texts, images, and controls; rather, the model must possess a thorough understanding of a GUI framework’s components, including the supported visual effects and compositions, to reproduce elements with the details (e.g., colors, fonts, margins) and positioning [13]. Thirdly, unlike static descriptions, the generated code must be executable, adhering to the syntax and semantic requirements of front-end frameworks.

To understand MLLMs’s capability in transforming screenshots to UI code, we conduct a motivating study to identify three main issues in this process: (1) element omission, where certain visual components are missing in the generated code, (2) element distortion, where elements are inaccurately reproduced in terms of shape, size, or color, and (3) element misarrangement, meaning the elements are not positioned or ordered correctly relative to their design layout. In contrast, when we cropped the inaccurately generated images into smaller pieces and asked MLLMs to re-generate UI code for each segment, we observed enhanced performance on these smaller, cropped screenshots. *In short, the smaller and more focused the image, the better the resulting code quality.*

Building on this insight, we propose a novel **Divide-and-Conquer**-based method to **Generate** website code from UI screenshots, namely **DCGen**. This end-to-end approach follows the principles of a typical divide-and-conquer algorithm: breaking down a complex problem into smaller parts, solving each part individually, and then combining the solutions to address the original problem. Specifically, DCGen consists of two phases: *division* and *assembly*. The

first phase involves slicing the screenshots into smaller, more manageable, yet semantically meaningful pieces, and generating the HTML and CSS code for each distinctive segment. The division aligns with the real-world front-end development practices [20] and is achieved via a novel image segmentation algorithm. DCGen then generates descriptions for each segment, followed by recursively reassembling these descriptions to reconstruct the entire website via UI code. This reassembly process is the reverse of the division procedure, where code from smaller, child segments is progressively integrated to build up their parent segments. This assembly continues until the full website structure is restored.

Our study curated a dataset comprising 1,000 top-ranked real-world websites. We evaluate the effectiveness of our methodology across several cutting-edge MLLMs, using 120 webpages sampled from the dataset. DCGen achieved up to 14% improvement in visual similarity between the original and generated websites compared to other design-to-code methods. We further demonstrate that DCGen is robust against various webpage complexities. Furthermore, DCGen is shown to generalize well across different MLLMs, demonstrating the effectiveness of the divide-and-conquer methodology.

In summary, our paper makes the following contributions:

- We initiated a motivating study to uncover types of errors in the LLM-powered design-to-code process, revealing the importance of visual segments in generation quality.
- We propose DCGen with a divide-and-conquer approach. It starts with generating descriptions for individual image segments, then merges these solutions to produce the complete UI code.
- The experiments on real-world webpages demonstrate the superiority of DCGen over other methods in both visual similarity and code similarity.
- We release all datasets and code implementation for future research in this field.

2 BACKGROUND

2.1 Concepts in Front-End Development

Front-end development concentrates on creating the user interface and enhancing the user experience of websites. It involves Hypertext Markup Language (HTML) for content structuring, Cascading Style Sheets (CSS) for styling, and optionally JavaScript for interactivity and dynamic webpage features.

2.1.1 HTML Elements & Tags. HTML is a markup language used in front-end web development to structure webpages. Tags in HTML define the document’s structure, like <h1> to <h6> for different heading levels, and <p> for paragraphs. Each HTML element includes an opening tag, content, and a closing tag, forming the basic block of a webpage. Below is a simplified HTML snippet containing six different elements:

```
<html>
<head>
  <title>Sample Page</title>
</head>
<body>
  <h1>Welcome to My Website</h1>
  <p>This is a paragraph of text.</p>
</body>
</html>
```

2.1.2 CSS. CSS is used in front-end web development to style webpages and enhance the appearance of HTML elements. It allows developers to define unique styles for elements through selectors, properties, and values. For example, to change the color and font size of all `<h1>` elements, one developer might write:

```
h1 {
  color: blue;
  font-size: 24px;
}
```

2.2 Problem Definition

Let C_0 be a file of HTML+CSS code of a webpage, I_0 be the screenshot of the webpage, and M be an MLLM. The *design-to-code* task takes the image I_0 as input and outputs a file of generated HTML+CSS code $C_g = M(I_0)$ that approximate C_0 . Figure 4 illustrates an example of the input and output. The quality of C_g is evaluated based on both functional similarity and visual similarity. Specifically, C_g should be functionally similar to C_0 , meaning it consists of a similar set of HTML elements and a comparable nested structure of the elements. Additionally, I_g , the screenshot of the webpage rendered from C_g , should be visually similar to I_0 .

3 DATASET COLLECTION

This section illustrates how we develop a dataset containing representative websites for this study. We randomly sample websites from the top 2,000 listed on the Tranco¹ [58], and process them until we have gathered 1,000 valid websites. First, we filter out all invalid websites (e.g., blocked, empty, or requiring human verification). Next, to make the websites self-contained and eliminate external dependencies that affect the UI code generation, we save each one into a single HTML file using the SingleFile toolkit², remove all external links, and replace images with placeholders. Finally, we clean the websites by removing all elements that do not impact the website’s appearance (i.e., hidden elements). The dataset collection yields 1,000 websites containing an average of 26 unique tags, where each HTML code file has an average length of 102,859 tokens.

Table 1 provides quantitative metrics to evaluate the complexity and comprehensiveness of our dataset. **(1) Length:** We tokenize the HTML code files in each category using the GPT-2 tokenizer. The average number of tokens is 102,859 (Min: 338, Max: 992,008, Std: 135,999), which suggests that our dataset covers a wide range of HTML code complexity. **(2) Total number of tags:** We counted the number of tags in HTML files, finding an average of 964 (Min: 1, Max: 16,331, Std: 1,370), which provides insights into the structural complexity of the documents. **(3) DOM tree depth:** We calculated the Document Object Model (DOM) tree depth in HTML files. The average depth is 17 (Min: 1, Max: 40, Std: 7), indicating the nesting complexity of HTML tags. **(4) Number of unique tags:** We also counted the number of unique tags, with an average of 26 (Min: 1, Max: 86, Std: 11), reflecting the diversity and content richness of the HTML files. Compared with existing datasets [11, 39, 62], our dataset is realistic and diverse in website complexity, making it well-suited for experiments in our paper.

¹<https://tranco-list.eu/>. Accessed in Jan 2024

²<https://github.com/gildas-lormeau/SingleFile>

Table 1: Statistics of the dataset.

	Min	Max	Average
Length (tokens)	338	992,008	102,859
Tag Count	1	16,331	1,370
DOM Depth	1	40	17
Unique Tags	1	86	26
Total size			1,000

To avoid data leakage, we select the top 12 websites for the motivating study and use the remaining ones for evaluation.

4 MOTIVATING STUDY

We begin with a motivating study to examine MLLMs’ ability to generate UI code from screenshots. Taking GPT-4o as an example, we showcase three common mistakes MLLMs make during the generation and further discuss how to mitigate these errors.

4.1 Study Preparation

To explore MLLM’s performance in the design-to-code task, we compare the original website’s appearance with the version generated by MLLM (i.e., GPT-4o in this section). This involves an image-based comparison to check if the *visual elements* from the original are accurately reproduced in the MLLM-generated website, after rendering.

4.1.1 Dataset sampling. The pilot study samples 12 top-ranked websites from the dataset described in Section 3, such as Amazon, Apple, and Facebook. After sampling, we prompt GPT-4o to generate website code from the screenshot using the direct prompt described in Section 6.1.4.

4.1.2 Visual Element Locating (for original websites). This step identifies the bounding boxes for each element (tag) in the code within the webpage screenshot, referred to as visual elements. Using Selenium WebDriver³, we extract the bounding box coordinates for all elements, then merge bounding boxes located in similar positions. We also eliminate any bounding boxes that intersect, as webpage elements typically do not overlap. This collection of bounding boxes enables us to locate all HTML elements in a website’s screenshot. Overall, these webpages contain a total of 1,699 HTML elements, with individual webpages featuring between 4 and 434 elements, averaging 142 elements per site.

4.2 What failures does MLLM produce when converting design to code?

We ask annotators to assess the accuracy of visual elements in MLLM-generated webpages compared to the original ones. Figure 1 illustrates the annotation interface. The annotators are provided with pairs of screenshots, with the original on the left and the MLLM-generated version on the right. A red bounding box highlights the visual element in the original screenshot. Annotators are asked with two tasks: (1) Drawing the bounding box around the corresponding element in the MLLM-generated screenshot. (2) Describing any differences between the generated visual element and the original in short phrases.

³<https://selenium-python.readthedocs.io/>

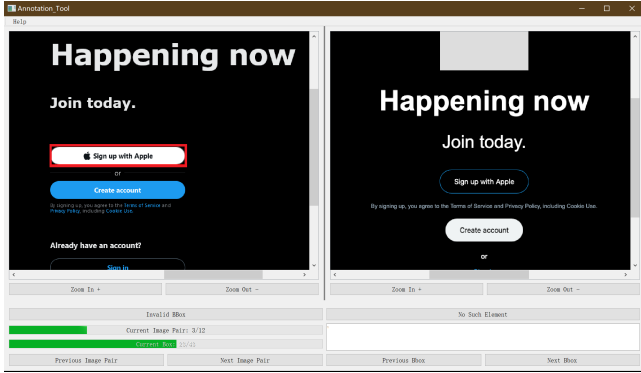
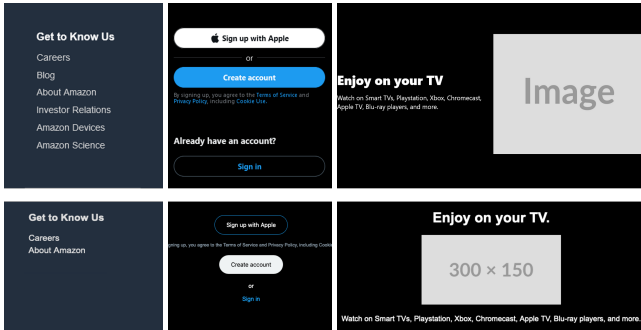


Figure 1: Annotation tool. Annotators are provided with an original webpage (left) with a bounding box specifying the visual element and a generated webpage (right).



(a) Omission (b) Distortion (c) Misarrangement

Figure 2: Examples of error cases (bottom).

After two annotators independently complete these tasks, we take the union of the two annotators’ descriptions as the final annotation for each element and manually analyze the descriptions.

Result Analysis. After inspection, we discover that all the differences between the generated element and the original element can be characterized into three categories, that is, element omission, element distortion, and element misarrangement, and one element can have multiple errors at the same time. Figure 5 provides an example of each type of error, with the original website displayed above and the MLLM-generated version below.

- (1) Element omission: Certain visual elements are missing in the generated code. As shown in Figure 2a, the text elements below “About Amazon” are missing.
- (2) Element distortion: Elements are reproduced inaccurately in terms of shape, size, or color. Figure 2b illustrates a case where the “sign up with Apple” button is incorrectly colored.
- (3) Element misarrangement: Elements are not positioned or ordered correctly relative to their adjacent elements or the overall design layout. In Figure 2c, MLLM misplaces the text “Enjoy on your TV” in relation to the image.

The distribution of these errors is shown in Table 2, showing that element omission accounts for the majority of error cases, which is potentially due to the visual shortcomings of MLLMs [64]. In total, MLLM correctly reproduces only 40 out of 1,699 elements, highlighting the need for a practical UI code generation approach.

Table 2: Distribution of common mistakes (one element can have multiple mistakes).

Category	Percentage (%)	Count
Omission	85.34	1,450
Distortion	2.56	44
Misarrangement	12.71	216
Same	2.35	40
Total		1,699

4.3 Can we correct mistakes by visual segments?

After noting the unsatisfactory performance in generating precise UI code, we became interested in understanding the reasons for these errors. LLMs are known to excel at simple, small-step tasks, and struggle with long-term planning for complex tasks [69]. To address this, existing studies have developed the Chain-of-Thought paradigm or LLM Agents, which decompose complex assignments into smaller, manageable sub-tasks, enabling models to perform more reasoning steps [29].

Inspired by these studies, we break down full screenshots into smaller image segments to investigate whether MLLMs perform better with simpler inputs. This approach helps us determine whether the model is fundamentally incapable of generating the content or if its mistakes can be alleviated. In specific, we conduct follow-up investigations on two failure cases.

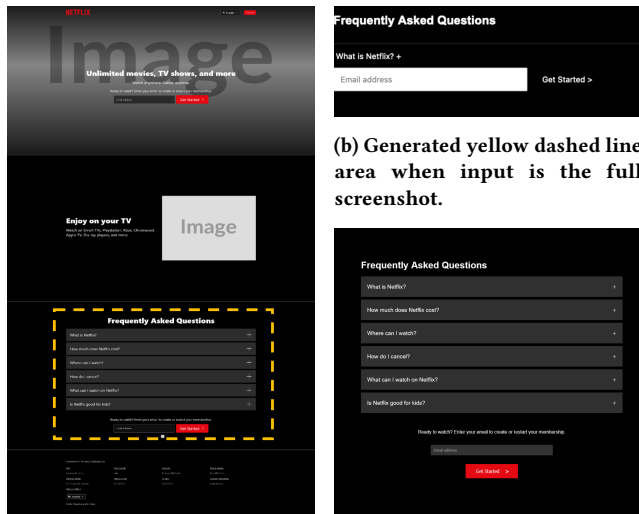
The first case focuses on omitted elements. We isolate each missing element by cropping the screenshot to include only that specific element and then request the model to generate the corresponding code. Figure 3 depicts this process, where Figure 3(b) is the Frequently Asked Questions (FAQ) area generated from the full screenshot and Figure 3(c) is the FAQ area generated from the cropped screenshot of the original FAQ area. The results show that with these isolated inputs, the model successfully generates the previously omitted content. This demonstrates that the model is intrinsically capable of producing the required outputs but struggles with complex inputs.

The second investigation concerns distorted and misarranged elements. We compare the image similarity between the original elements and the model-generated elements from both full and cropped screenshots. We measure image similarity using the CLIP embeddings [59], as outlined in [62]. The findings reveal an overall improvement in similarity scores from 73.7% to 76.0% by providing the cropped screenshot, confirming that smaller and more focused images can enhance the quality of the generated code.

Insights: While existing MLLMs struggle with generating accurate UI code, we observe that breaking down full screenshots into smaller visual segments improves performance. This decomposition allows models to conduct more reasoning steps, each focused on a manageable sub-generation task.

5 METHODOLOGY

In this section, we present DCGen, an end-to-end framework for automated UI code generation from screenshots. Motivated by the



(a) Input. The full image is the input of (b) and the yellow dashed line area is the input of (c).
 (b) Generated yellow dashed line area when input is the full screenshot.
 (c) Generated yellow dashed line area when input is the area's screenshot.

Figure 3: An example of the experiment in the motivating study.

traditional “*divide and conquer*” algorithmic technique, DCGen decomposes a complicated screenshot into smaller, doable visual segments, solves each part individually, and then combines the solutions for the original problem.

DCGen accepts website screenshots and outputs a file of UI Code. Figure 4 shows the overall workflow of DCGen, consisting of two stages: *division* and *assembly*. In the division stage, DCGen segments the screenshot recursively into smaller pieces. Specifically, DCGen first searches for horizontal separation lines in a webpage and splits the image accordingly. For each horizontal segment, DCGen then looks for vertical separation lines and further divides the segment. This recursive “horizontal then vertical splitting” process continues, breaking the image into smaller, complete pieces until no more separation lines are found or a user-defined maximum depth is reached. At this point, DCGen passes each image segment to MLLMs for code generation. Afterward, in the assembly stage, code from smaller, child segments is progressively integrated to build up their parent segments. This recursive assembly continues until the full structure of the website is restored.

5.1 Division

Given a full screenshot, the division stage outputs a hierarchical structure of image separations, with each leaf node representing a fully subdivided image (i.e., the smallest segment). The screenshot division faces two challenges. First, the division algorithm must carefully examine visual elements to ensure that no single element is split into multiple segments. Second, the image segments should be stored in order, so that they can be reconstructed for the full webpage later.

The following section delineates a novel division algorithm, which comprises two main components: separation line detection and screenshot subdivision. The separation line detector first identifies all explicit or implicit separation lines within screenshots (either

vertical or horizontal). Then, the screenshot subdivision component leverages these lines to segment the image into smaller and hierarchical segments. The two components work alternately, dividing the image horizontally, then vertically for the subimages, and again horizontally for the sub-subimages. Figure 5 illustrates various outcomes of the screenshot segmentation algorithm at different depths (i.e., the number of alternations).

5.1.1 Separation Line Detection. DCGen starts with identifying all separation lines (either vertical or horizontal) in a full screenshot. These separation lines must divide the screenshot into rectangular and meaningful pieces, where each of the pieces contains complete elements; otherwise, it would be more difficult to combine code for fractured pieces later. Traditional image segmentation techniques concentrate on distinguishing irregularly shaped objects from the background [48], becoming unsuitable for dividing webpages.

We observe that websites contain explicit (visible lines separating content) or implicit (blank spaces or borders between content elements) separation lines to organize different sections and contents. Figure 6 depicts examples of both types. The left figure employs explicit lines to separate the grey area from the purple area, while the right figure adapts implicit lines to arrange text sections.

Motivated by two types of separation lines, our algorithm (shown in Algorithm 1) begins by converting the screenshot to grayscale, and then scans the screenshot row by row to identify explicit lines and implicit lines, respectively. The separation lines are signified by sudden shifts in pixel values.

For detecting implicit separation lines, our approach incorporates a sliding window technique (lines 3-5), analyzing groups of consecutive rows to detect zones of minimal brightness variation, indicating potential blank spaces (lines 6-7). The algorithm compares each window against the rows directly above and below (lines 8-11). A separation line is identified if (1) the variance within the window is lower than a set threshold, suggesting a blank area, and (2) the brightness difference between this window and the rows directly above and below exceeds another threshold over more than 30% of the row’s length (line 12). This dual-threshold method facilitates the identification of subtle borders and blanks, recognizing both the low-content areas and the significant transitions at their edges. The thresholds and parameters used in the algorithm are manually optimized on a subset of our dataset.

For detecting explicit separation lines, the method is equivalent to finding implicit separation lines by setting the sliding window size to one. In particular, the algorithm scrutinizes each row for uniformity in pixel brightness. A row with variability below a predefined threshold is flagged as a potential line. Confirmation of a separation line occurs if the average difference in brightness between this row and its predecessor or successor surpasses a set threshold over at least 30% of the row.

5.1.2 Screenshot Subdivision. We divide the screenshot into smaller segments by *alternately and recursively* applying horizontal and vertical divisions. Specifically, for each input screenshot, DCGen first attempts to divide the screenshot along horizontal separation lines. If no such lines are detected, it then proceeds to segment the screenshot using vertical separation lines by calling the separation line detector again. This process is applied recursively to each

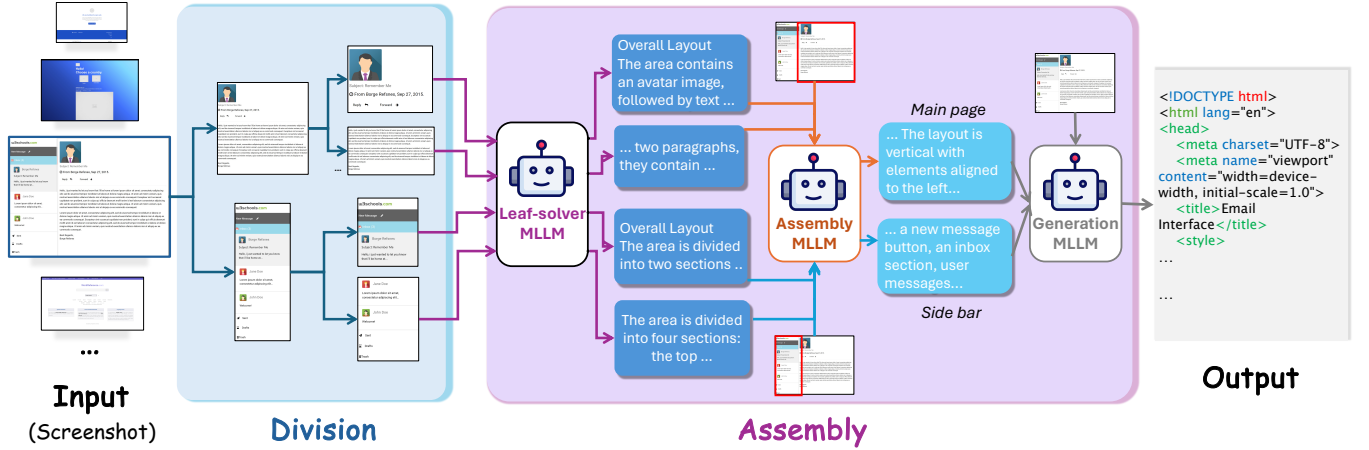


Figure 4: The framework of DCGen.

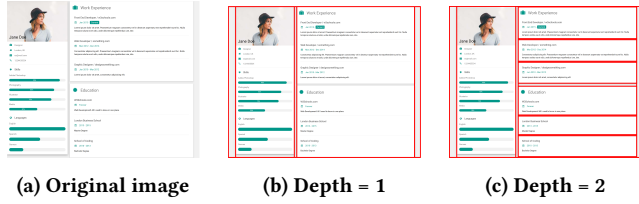


Figure 5: Examples of image subdivision of different depths.

Algorithm 1 Separation Line Detection Algorithm

Require: img , var_thr , $diff_thr$, $portion_thr$, $window_size$

- 1: $lines \leftarrow []$
- 2: **for** $i \leftarrow window_size + 1$ **to** $len(img) - 1$ **do**
- 3: $upper \leftarrow img[i - window_size - 1]$
- 4: $window \leftarrow img[i - window_size : i]$
- 5: $lower \leftarrow img[i]$
- 6: $var \leftarrow variance(window)$
- 7: $is_blank \leftarrow (var < var_thr)$
- 8: $diff_top \leftarrow mean_abs_diff(upper, window[0])$
- 9: $is_border_top \leftarrow (diff_top > diff_thr \text{ and } portion(diff_top) > portion_thr)$
- 10: $diff_bottom \leftarrow mean_abs_diff(lower, window[-1])$
- 11: $is_border_bottom \leftarrow (diff_bottom > diff_thr \text{ and } portion(diff_bottom) > portion_thr)$
- 12: **if** is_blank **and** $(is_border_top \text{ or } is_border_bottom)$ **then**
- 13: **if** is_border_bottom **then**
- 14: $pos \leftarrow i$
- 15: **else**
- 16: $pos \leftarrow i - window_size$
- 17: **end if**
- 18: $lines.append(pos)$
- 19: **end if**
- 20: **end for**
- 21: **return** $sorted(lines)$

resulting segment until no further separation lines can be identified, or until a user-defined maximum recursion depth is reached. Figure 7 illustrates this subdivision procedure.

We employ a tree structure to store the hierarchical screenshot divisions. If the image I is divided into segments I_a and I_b , then I is

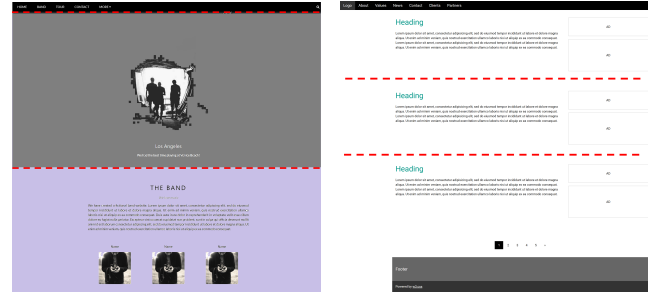


Figure 6: Separation lines (marked with red dot line).

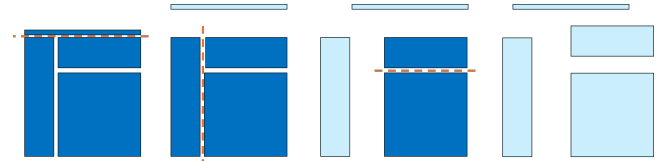


Figure 7: Screenshot subdivision example.

considered the parent of segments I_a and I_b , with I_a and I_b as its children. Consequently, the number of recursions corresponds to the number of layers in the tree. Each leaf node represents a fully subdivided screenshot, which is the smallest segment.

5.2 Assembly

In the assembly process, we integrate the solutions of image subdivisions to generate complete UI code for the original screenshot. The assembly process is essentially the reverse of the division procedure, where code from smaller, child segments is progressively integrated to build up their parent segments. This recursive assembly continues until the full structure of the website is restored.

As shown in Figure 4, for each leaf image segment, DCGen provides the MLLM (i.e., Leaf-solver MLLM) a website screenshot with a red rectangular bounding box specifying the part of the image it should focus on, then ask it to describe the image segment.

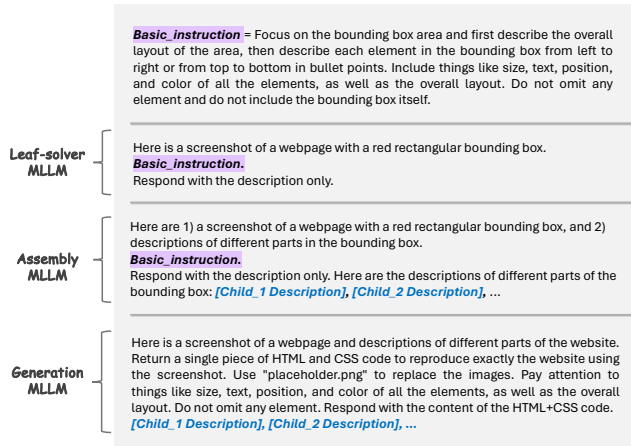


Figure 8: Prompt details for the leaf-solver MLLM, assembly MLLM, and generation MLLM, respectively.

For each parent image segment, DCGen provides the MLLM (i.e., Assembly MLLM) a screenshot with a bounding box, as well as all the descriptions generated from its children’s image segments. In the last step (merging for root node), DCGen calls the Generation MLLM to produce the complete UI code for full screen, based on the descriptions from its children segments.

Figure 8 illustrates the prompt details for the leaf-solver MLLM, assembly MLLM, and generation MLLM, respectively. We adapt the basic instructions based on the previous study by Si et al. [62].

6 EXPERIMENT

We evaluate the effectiveness of DCGen for the design-to-code performance by answering the following research questions.

- **RQ1:** How does DCGen perform in design-to-code generation compared to various direct prompting strategies?
- **RQ2:** Which language modality (e.g., programming language or natural language) maximizes the performance of DCGen?
- **RQ3:** How does the complexity of real-world websites impact the performance of DCGen?
- **RQ4:** Can DCGen be generalized to other state-of-the-art (SOTA) MLLMs?

6.1 Experiment Setup

6.1.1 Backbone Models. To assess the performance of DCGen, we employ it to evaluate three SOTA MLLMs: GPT-4o [55], Gemini-1.5 [32], Claude-3 [7]. Access to all models is facilitated through their respective official APIs, the specific model numbers are 20240513 for GPT-4o, 20240229 for Claude-3-Sonnet, and Gemini-1.5-flash-latest accessed during May 2024. We randomly sampled 120 websites from our dataset to form the testing set. Table 3 shows the statistics of the testing dataset, the data is rich in HTML tags and diverse in overall complexity.

6.1.2 Parameter Setting. For MLLM model configurations, we set the temperature to 1, and the *max_tokens* parameter to the maximum allowable value for each model (i.e., 4096 for GPT-4o and

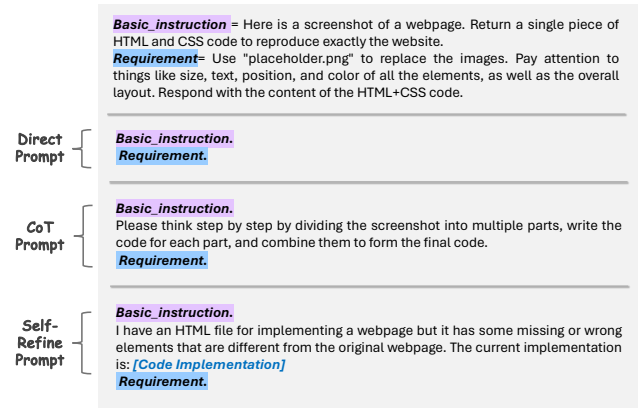


Figure 9: Prompt for baseline approaches.

Table 3: Statistics of the test data

	Min	Max	Average
Length (tokens)	338	992,008	41,264
Tag Count	1	397	175
DOM Depth	1	34	12
Unique Tags	1	57	17
Total size			120

Claude3-Sonnet, 8192 for Gemini-1.5-Flash), while other parameters are maintained at their default settings as specified in the corresponding API documentation [8, 33, 56]. For parameters in the image segmentation algorithm, we set *var_thr=60*, *diff_thresh=5*, *diff_portion=0.3*, and set the division depth to one.

6.1.3 Efficiency. Our experiments were conducted on a Windows 10 PC with an IntelCore i7-10870H CPU. We assess the performance of DCGen by first evaluating the speed of the Image subdivision algorithm, which completes the subdivision of a 1920x1080 pixel image in less than one second when the division depth is set to one. The response times for API requests across three models range from 5 to 15 seconds depending on the request length. On average, DCGen generates code for an entire webpage (1,370 tags) within 12 minutes, significantly faster than a person typing the tags manually [66]. The leaf-solver MLLMs could work in parallel for (10x) faster computation, theoretically. This demonstrates DCGen’s practical efficiency in accelerating web development.

6.1.4 Baselines. Figure 9 illustrates the details of prompting strategies used in our experiment as baselines. Chain-of-Thought (CoT) prompting [68] generates a chain of thought for each question and then generates the corresponding code. For CoT, we use the "let’s think step by step" instruction from Chae et al. [12]. Self-refine prompting [19] let the model refine its own generated code. We adopt the self-refine prompting and direct promoting method from Si et al. [62]. We do not select previous deep-learning-based approaches as baselines since they are either tailored to the mobile app environment [13, 49, 52], not opensourced [71], do not take website screenshot as input or do not produce complete website code [10, 11].

6.2 Metrics

Let C_0 be the original HTML+CSS code of the website, I_0 be the screenshot of the original website, and C_g, I_g be the code and screenshot of the generated website. We evaluate the performance of DCGen in both high-level similarity and fine-grained element matching.

6.2.1 High-Level Similarity. We utilize two high-level similarities in this paper including **code similarity** and **image similarity**, respectively.

For **code similarity**, we adopt the Bilingual Evaluation Understudy (BLEU) score [57] to evaluate the closeness of generated code C_g to the original code C_0 . BLEU score is an automatic evaluation metric widely used in machine translation studies. It calculates the similarity of machine-generated translations and human-created references (i.e., ground truth). It is also widely used in code generation tasks to measure the similarity between generated code and the ground truth [16, 45, 60, 67, 73]. BLEU score is defined as the product of n-gram precision and a brevity penalty BP : $BLEU = BP \cdot \exp\left(\sum_{n=1}^N w_n \log p_n\right)$, where p_n is the precision of the n-grams, w_n is the weight (typically $\frac{1}{N}$), and N is usually set to 4 [63]. BP is 1 if the candidate translation length c exceeds the reference length r , and $\exp\left(1 - \frac{c}{r}\right)$ otherwise. BLEU scores range from 0 to 1, with higher scores indicating closer similarity to the reference translations.

For **image similarity**, we measure image similarity between I_0 and I_g via CLIP Score [62]. CLIP score relies on the similarity of their CLIP [59] embeddings, denoted as $CLIP(I_0, I_g)$. Specifically, we extract features using CLIP-ViT-B/32 after resizing the screenshots to squares. To eliminate noise introduced by text in the screenshots, we mask all detected text boxes using their bounding box coordinates with an inpainting algorithm implemented in OpenCV⁴.

6.2.2 Fine-Grained Measurements. High-level metrics capture only the overall similarity of images and code, lacking the detail necessary to analyze specific model performances. To address this limitation, we adopt a suite of element-matching metrics for evaluating generated webpages in terms of text content, position, and color introduced by Si et al. [62]. Given reference and generated webpage screenshots I_0 and I_g , the algorithm detects visual element blocks and matches them using the Jonker-Volgenant algorithm. It then evaluates the similarity of the matching blocks across several aspects: (1) **Block-match** measures the ratio of matched block sizes to all block sizes, penalizing missing or hallucinated blocks; (2) **Text similarity** calculates character overlap using the Sørensen-Dice coefficient; (3) **Color similarity** employs the CIEDE2000 formula to evaluate perceptual color differences; and (4) **Position similarity** assesses the alignment of block centers. We use this set of metrics as indicators for the three types of errors found in Section 4. Specifically, we use (1) for measuring element **inclusion** (omission), (2) and (3) for measuring element **fidelity** (distortion), and (4) for indicating element **organization** (misarrangement).

Table 4: GPT-4o high-level performance (%)

Method	CLIP	BLEU
Direct	69.94	6.78
CoT	62.52	6.20
Self-Refine	75.19	7.91
DCGen (Ours)	83.36	8.17

7 RESULTS & ANALYSIS

7.1 RQ1: Effectiveness of DCGen

This RQ assesses DCGen’s performance in design-to-code generation by comparing it against various direct prompting strategies across multiple metrics.

High-level performance. Table 4 presents the overall performance of various methods evaluated on the CLIP and BLEU metrics tested on GPT-4o. The results indicate that DCGen achieves the most substantial performance gains in both metrics. Notably, while DCGen and the self-refine approach contribute positively to model performance, the Chain-of-Thought (CoT) prompting approach has a negative impact on the model’s capabilities. Further analysis of the code generated under CoT instruction shows that 70% (84 out of 120) of HTML files contain no CSS content, leading to the generation of purely textual websites devoid of color or style, which indicates the step-by-step visual reasoning procedure impedes the instruction following ability of the model.

Fine-grained metrics. As detailed in Figure 10, DCGen surpasses both the direct-prompt approach and CoT instruction in fine-grained metrics. DCGen and the self-refine approach enhance GPT-4o’s performance across all metrics, notably in text, color, and block-match metrics, which are indicators of element inclusion and fidelity. Specifically, our method excels in color and block similarity than the self-refine approach. Conversely, while CoT instruction enhances text similarity, it detrimentally affects the model’s ability to reproduce colors, resulting in decreased element fidelity. This observation underscores a significant limitation: current MLLMs struggle with complex visual tasks when left to operate autonomously. The enhanced performance of our method suggests that providing MLLMs with more precise and focused information, such as focused images and fine-grained descriptions, significantly boosts their effectiveness. Figure 11 illustrates two webpage cases (i.e., top and bottom) generated by multiple approaches, demonstrating the superiority of DCGen.

Answer to RQ1: DCGen consistently outperforms other design-to-code techniques on both high-level and fine-grained metrics, due to the precise and focused image segments.

7.2 RQ2: Influence of Language Modality

Drawing inspiration from Chae et al. [12, 17], which suggests that programming language (PL) may enhance LLMs’ reasoning ability

⁴https://docs.opencv.org/4.3.0/df/d3d/tutorial_py_inpainting.html

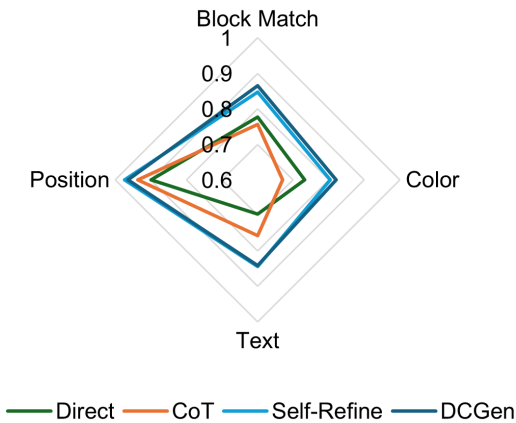


Figure 10: Fine-grained metrics

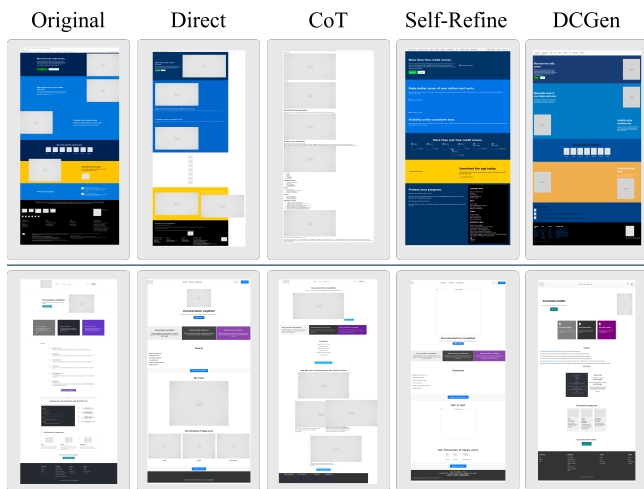


Figure 11: Two examples of visual comparison of original and generated websites.

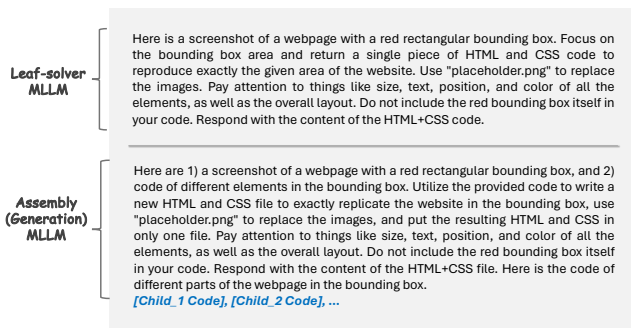


Figure 12: Prompt details for code-base intermediate description for DCGen.

than natural language (NL), we thus investigate which language modality maximizes DCGen’s performance in RQ2.

Table 5: Performance metrics across language modality (%).

Model	CLIP	BLEU	Block Match	Position	Text	Color
GPT4-NL	83.36	8.17	86.54	96.49	84.11	82.13
GPT4-PL	84.93	7.87	88.14	97.53	85.41	83.93
Gemini-NL	77.63	8.81	84.15	96.85	84.30	75.97
Gemini-PL	78.76	8.30	83.81	97.02	81.88	75.58

To answer this RQ, we compare different implementations of DCGen in terms of language modality. In particular, instead of letting MLLMs generate intermediate descriptions for image subdivisions, we directly let the models translate the screenshot segments to code and then perform the assembly process. Prompt details are illustrated in Figure 12. Since UI code has been the intermediate description in DCGen, the assembly MLLM would serve the same role as the generation MLLM and utilize the same prompt.

We investigate the effectiveness of using programming language (PL) versus natural language (NL) in implementing DCGen on two models, GPT-4o and Gemini-1.5-Flash, with the results presented in Table 5. Our results indicate that for GPT-4o, employing PL consistently enhances performance across all visual metrics compared to NL. However, both methods yield similar outcomes for Gemini. The differential performance can potentially be attributed to two factors. Firstly, existing research [12, 17] suggests that integrating coding into the reasoning process enhances the ability of LLMs to tackle complex tasks. Specifically, by generating accurate code snippets for image segments and subsequently merging them to reconstruct complete website code, MLLMs are more likely to produce precise outputs. Conversely, our observations during the experiments revealed a potential drawback: smaller coding errors tend to propagate and accumulate during the assembly process, more so than with NL descriptions. This error propagation can preserve initial mistakes throughout the assembly process, ultimately compromising the overall quality of the reconstructed website. This phenomenon potentially explains why PL implementation does not always surpass NL implementation.

Answer to RQ2: Although PL implementation can enhance GPT-4o’s performance on all visual metrics, minor coding errors would accumulate in assembly more than with NL descriptions. As a result, the best language modality depends on the specific model.

7.3 Influence of Website Complexity

Recognizing the diverse complexity of real-world websites, this RQ evaluates DCGen’s efficacy on websites with varying complexity levels. We quantify website complexity using the number of HTML tags and focus on changes in three key metrics as functions of website complexity on GPT-4o: CLIP score, BLEU score, and the average of all four fine-grained metrics (Block Match, Text, Position, Color). Figure 13, Figure 14, and Figure 15 illustrate how these metrics vary with website complexity. We observe that DCGen consistently achieves leading performance across all complexity levels for each metric evaluated. Notably, DCGen demonstrates a strong ability to maintain high visual scores (i.e., CLIP and average fine-grain

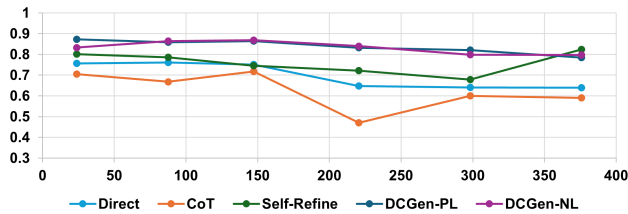


Figure 13: CLIP score versus website complexity.

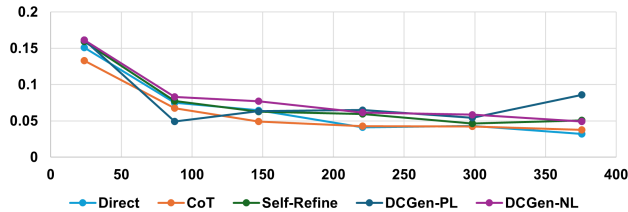


Figure 14: BLEU score versus website complexity.

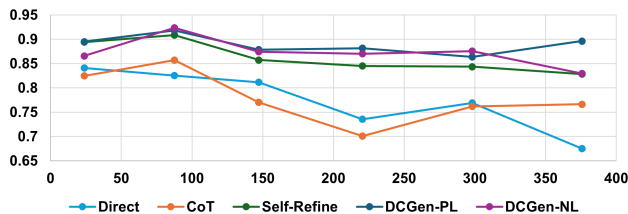


Figure 15: Average fine-grain score versus website complexity.

score), indicating its effectiveness in producing code implementations that visually resemble the original webpages, regardless of their complexity. This performance suggests that DCGen is robust to variations in website complexity, effectively handling both simple and intricate website structures.

Answer to RQ3: DCGen delivers superior performance across various website complexities, indicating its robustness in handling both simple and intricate webpages.

7.4 Generalization of DCGen

In this RQ, we examine the generalizability of DCGen by employing the methodology on different MLLMs as backbones. Tables 6 and 7 display the overall performance of DCGen on these MLLMs. Our results indicate that DCGen is highly adaptable to the Gemini model, achieving notable gains in both visual level and code level metrics compared to other methods. For the Claude-3 platform, DCGen significantly enhances the visual similarity between the original and the generated websites, outperforming competing methods.

Answer to RQ4: DCGen is effective across different MLLMs in generating UI code from design, which demonstrates the generalizability of the proposed divide-and-conquer strategy.

Table 6: Gemini result.

Gemini	CLIP	BLEU
Direct	72.01	8.46
CoT	72.10	8.65
Self-Refine	73.74	8.44
DCGen	77.63	8.81

Table 7: Claude-3 result.

Claude-3	CLIP	BLEU
Direct	73.77	5.94
CoT	73.21	5.99
Self-Refine	77.85	8.17
DCGen	81.68	6.00

8 THREAT TO VALIDITY

Limited context length. Current MLLMs have constraints on the length of the context window (e.g., 128K for GPT-4o). Consequently, our approach may fail to handle websites that require a vast number of tokens, exceeding the capacities of MLLMs. Nevertheless, our experiment demonstrates that all of the prompts is below the maximum context length, showing our approach is generalizable for most scenarios.

The selection of backbone models. This study employs three popular instruction-following and multimodal LLMs to demonstrate the effectiveness of DCGen. While other LLMs might be adapted for our methodology, we found that smaller parameter models fail to understand complex prompts. Our future work involves extending our implementation to other emerging models, showcasing DCGen’s generalization abilities.

Unable to handle dynamic websites. Some websites incorporate dynamic features to enhance user interaction, modifying webpage content using server-side scripting languages (e.g., PHP, Python). Although DCGen can only handle static webpages, it is the first segment-aware approach to generate UI code from screenshots, which we believe is an important step toward creating complex dynamic websites.

9 RELATED WORK

9.1 Image-to-code Generation

The most informative AI techniques used for generating code from images can be classified into three broad categories: (i) Convolutional Neural Networks (CNNs) [10, 11, 13, 18, 22, 49, 71], (ii) Computer Vision (CV) and Optical Character Recognition (OCR) [51, 52], and (iii) other deep learning models [5, 70]. The work [11] utilizes CNNs and LSTM to extract features from GUI images to generate a domain-specific language (DSL). However, DSLs are not widely used in practical development, which inconveniences the industry’s UI developers [71]. An alternative approach [13] using CNNs to extract visual features from UI images is more widely applicable than generating fixed DSL code. Based on CNNs, Andre et al. [22] pioneered using Class Activation Mapping (CAM), further improving the performance and interpretability of the image-to-code generation task.

9.2 Multimodal Language Models

Multimodal Language Models (MLLM) refer to LLM-based models capable of receiving, reasoning, and outputting multimodal information [74]. In recent years, the trend of using LLMs as decoders in vision-language tasks has gained significant traction. This approach leverages cross-modal transfer, enabling knowledge sharing between language and multimodal domains. Pioneering studies

such as VisualGPT [15] and Frozen [65] have demonstrated the advantages of employing a pre-trained language model as a decoder. Following this, Flamingo [6] was developed to align a pre-trained vision encoder and language model using gated cross-attention, and it was trained on billions of image-text pairs, showcasing impressive in-context few-shot learning capabilities. Furthermore, BLIP-2 [41] introduced the use of Flan-T5 [21] with a Q-Former to efficiently align visual features with the language model. PaLM-E [27], featuring 562 billion parameters, was developed to integrate real-world continuous sensor modalities into an LLM, establishing a connection between real-world perceptions and human languages. Additionally, GPT-4 [54] demonstrates enhanced visual understanding and reasoning abilities following pre-training on a vast collection of aligned image-text data. More recently, GPT-4o was proposed [55] to achieve more effective and efficient image understanding and reasoning.

10 CONCLUSION

In this paper, we first present a motivating study that identifies prevalent failures in MLLMs during the design-to-code generation process. Drawing on these insights, we design and implement DC-Gen, a novel divide-and-conquer-based framework for effectively generating UI code from web screenshots. We evaluate DCGen across three SOTA MLLMs and demonstrate that it consistently outperforms various direct prompting strategies. Furthermore, DC-Gen shows robustness against variations in website complexity and is generalizable across different MLLMs, demonstrating its superiority in generating UI code.

REFERENCES

- [1] 2024. 17+ Surprising WordPress Statistics You Should Not Miss [2024]. *WPDeveloper* (2024). <https://wpdeveloper.com/wordpress-statistics-2024> Accessed: 2024-05-30.
- [2] 2024. Differences Between Mobile App and Web Development. *KnowledgeHut* (2024). <https://www.knowledgehut.com/blog/programming/differences-mobile-app-web-development>
- [3] 2024. How Many Websites Are There in 2024? (13 Latest Statistics). *TechJury* (2024). <https://techjury.net/blog/how-many-websites-are-there/> Accessed: 2024-05-30.
- [4] 2024. Website & Mobile App Design: Differences In 2024? *Inkbot Design* (2024). <https://inkbotdesign.com/differences-website-mobile-app-design/>
- [5] A. A. Abdelhamid, S. R. Alotaibi, and A. Mousa. 2020. Deep learning-based prototyping of android GUI from hand-drawn mockups. *IET Software* 14, 7 (2020), 816–824.
- [6] Jean-Baptiste Alayrac, Jeff Donahue, Pauline Luc, Antoine Miech, Iain Barr, Yana Hasson, Karel Lenc, Arthur Mensch, Katherine Millican, Malcolm Reynolds, et al. 2022. Flamingo: a visual language model for few-shot learning. *Advances in neural information processing systems* 35 (2022), 23716–23736.
- [7] Anthropic. 2024. Claude. <https://www.anthropic.com/claude> Accessed: 2024-06-06.
- [8] Anthropic. 2024. Vision Documentation. <https://docs.anthropic.com/en/docs/vision> Accessed: 2024-06-06.
- [9] Shushan Arakelyan, Rocktim Jyoti Das, Yi Mao, and Xiang Ren. 2023. Exploring Distributional Shifts in Large Language Models for Code Analysis. In *Conference on Empirical Methods in Natural Language Processing*. <https://api.semanticscholar.org/CorpusID:257557735>
- [10] Batuhan Asiroglu, Büşta Rümeyza Mete, Eyyüp Yildiz, Yagiz Nalçakan, Alper Sezen, Mustafa Dağtekin, and Tolga Ensari. 2019. Automatic HTML Code Generation from Mock-Up Images Using Machine Learning Techniques. *2019 Scientific Meeting on Electrical-Electronics & Biomedical Engineering and Computer Science (EBBT)* (2019), 1–4. <https://api.semanticscholar.org/CorpusID:195223316>
- [11] T. Beltramelli. 2018. pix2code: Generating code from a graphical user interface screenshot. In *Proceedings of the ACM SIGCHI Symposium on Engineering Interactive Computing Systems*. 1–6.
- [12] Hyungjoo Chae, Yeonghyeon Kim, Seungone Kim, Kai Tzu iunn Ong, Beong woo Kwak, Moohyeon Kim, Seonghwan Kim, Taeyoon Kwon, Jiwan Chung, Youngjae Yu, and Jinyoung Yeo. 2024. Language Models as Compilers: Simulating Pseudocode Execution Improves Algorithmic Reasoning in Language Models. *ArXiv abs/2404.02575* (2024). <https://api.semanticscholar.org/CorpusID:268876471>
- [13] C. Chen, T. Su, G. Meng, Z. Xing, and Y. Liu. 2018. From UI design image to GUI skeleton: a neural machine translator to bootstrap mobile GUI implementation. In *Proceedings of the 40th International Conference on Software Engineering*. 665–676.
- [14] Fuxiang Chen, Fateme Moradian Fard, David Lo, and Timofey Bryksin. 2022. On the Transferability of Pre-trained Language Models for Low-Resource Programming Languages. *2022 IEEE/ACM 30th International Conference on Program Comprehension (ICPC)* (2022), 401–412. <https://api.semanticscholar.org/CorpusID:248266381>
- [15] Jun Chen, Han Guo, Kai Yi, Boyang Li, and Mohamed Elhoseiny. 2022. Visualgpt: Data-efficient adaptation of pretrained language models for image captioning. In *Proceedings of the IEEE/CVF Conference on Computer Vision and Pattern Recognition*. 18030–18040.
- [16] Mark Chen, Jerry Tworek, Heewoo Jun, Qiming Yuan, Henrique Ponde, Jared Kaplan, Harrison Edwards, Yura Burda, Nicholas Joseph, Greg Brockman, Alex Ray, Raul Puri, Gretchen Krueger, Michael Petrov, Heidy Khlaaf, Girish Sastry, Pamela Mishkin, Brooke Chan, Scott Gray, Nick Ryder, Mikhail Pavlov, Alethea Power, Lukasz Kaiser, Mohammad Bavarian, Clemens Winter, Philippe Tillet, Felipe Petroski Such, David W. Cummings, Matthias Plappert, Fotios Chantzis, Elizabeth Barnes, Ariel Herbert-Voss, William H. Guss, Alex Nichol, Igor Babuschkin, Suchir Balaji, Shantanu Jain, Andrew Carr, Jan Leike, Joshua Achiam, Vedant Misra, Evan Morikawa, Alec Radford, Matthew M. Knight, Miles Brundage, Mira Murati, Katie Mayer, Peter Welinder, Bob McGrew, Dario Amodei, Sam McCandlish, Ilya Sutskever, and Wojciech Zaremba. 2021. Evaluating Large Language Models Trained on Code. *ArXiv abs/2107.03374* (2021). <https://api.semanticscholar.org/CorpusID:235755472>
- [17] Wenhu Chen, Xueguang Ma, Xinyi Wang, and William W. Cohen. 2022. Program of Thoughts Prompting: Disentangling Computation from Reasoning for Numerical Reasoning Tasks. *ArXiv abs/2211.12588* (2022). <https://api.semanticscholar.org/CorpusID:253801709>
- [18] W.-Y. Chen, P. Podstreleny, W.-H. Cheng, Y.-Y. Chen, and K.-L. Hua. 2022. Code generation from a graphical user interface via attention-based encoder–decoder model. *Multimedia Systems* 28, 1 (2022), 121–130.
- [19] Xinyun Chen, Maxwell Lin, Nathanael Schärli, and Denny Zhou. 2023. Teaching Large Language Models to Self-Debug. *ArXiv abs/2304.05128* (2023). <https://api.semanticscholar.org/CorpusID:258059885>
- [20] CSS Chopper. 2024. *How to Convert PSD to HTML: A Complete Guide*. <https://www.csschopper.com/blog/how-to-convert-psd-to-html-a-complete-guide/> Accessed: 31-05-2024.
- [21] Hyung Won Chung, Le Hou, Shayne Longpre, Barret Zoph, Yi Tay, William Fedus, Yunxuan Li, Xuezhi Wang, Mostafa Dehghani, Siddhartha Brahma, et al. 2024. Scaling instruction-finetuned language models. *Journal of Machine Learning Research* 25, 70 (2024), 1–53.
- [22] A. A. J. Cizotto, R. C. T. de Souza, V. C. Mariani, and L. dos Santos Coelho. 2023. Web pages from mockup design based on convolutional neural network and class activation mapping. *Multimedia Tools and Applications* (2023), 1–27.
- [23] Wenliang Dai, Junnan Li, Dongxu Li, Anthony Meng Huat Tiong, Junqi Zhao, Weisheng Wang, Boyang Albert Li, Pascale Fung, and Steven C. H. Hoi. 2023. InstructBLIP: Towards General-purpose Vision-Language Models with Instruction Tuning. *ArXiv abs/2305.06500* (2023). <https://api.semanticscholar.org/CorpusID:258615266>
- [24] Victor C. Dibia, Adam Fourney, Gagan Bansal, Forough Poursabzi-Sangdeh, Han Liu, and Saleema Amershi. 2022. Aligning Offline Metrics and Human Judgments of Value of AI-Pair Programmers. *ArXiv abs/2210.16494* (2022). <https://api.semanticscholar.org/CorpusID:253237523>
- [25] Hantian Ding, Varun Kumar, Yuchen Tian, Zijian Wang, Robert Kwiatkowski, Xiaopeng Li, Murali Krishna Ramanathan, Baishakhi Ray, Parminder Bhatia, Sudipta Sengupta, Dan Roth, and Bing Xiang. 2023. A Static Evaluation of Code Completion by Large Language Models. *ArXiv abs/2306.03203* (2023). <https://api.semanticscholar.org/CorpusID:259088657>
- [26] Yihong Dong, Xue Jiang, Zhi Jin, and Ge Li. 2023. Self-collaboration Code Generation via ChatGPT. *ArXiv abs/2304.07590* (2023). <https://api.semanticscholar.org/CorpusID:258179537>
- [27] Danny Driess, Fei Xia, Mehdi SM Sajjadi, Corey Lynch, Aakanksha Chowdhery, Brian Ichter, Ayzan Wahid, Jonathan Tompson, Quan Vuong, Tianhe Yu, et al. 2023. PaLM-E: An Embodied Multimodal Language Model. In *International Conference on Machine Learning*. PMLR, 8469–8488.
- [28] Xueying Du, Mingwei Liu, Kaixin Wang, Hanlin Wang, Junwei Liu, Yixuan Chen, Jiayi Feng, Chaofeng Sha, Xin Peng, and Yiling Lou. 2023. ClassEval: A Manually-Crafted Benchmark for Evaluating LLMs on Class-level Code Generation. *ArXiv abs/2308.01861* (2023). <https://api.semanticscholar.org/CorpusID:260439062>
- [29] Sidong Feng and Chunyang Chen. 2024. Prompting Is All You Need: Automated Android Bug Replay with Large Language Models. In *Proceedings of the 46th IEEE/ACM International Conference on Software Engineering*. 1–13.
- [30] Shuzheng Gao, Xinjie Wen, Cuiyun Gao, Wenxuan Wang, and Michael R. Lyu. 2023. Constructing Effective In-Context Demonstration for Code Intelligence Tasks: An Empirical Study. *ArXiv abs/2304.07575* (2023). <https://api.semanticscholar.org/CorpusID:258179537>

- //api.semanticscholar.org/CorpusID:263867793
- [31] Henry Gilbert, Michael Sandborn, Douglas C. Schmidt, Jesse Spencer-Smith, and Jules White. 2023. Semantic Compression with Large Language Models. *2023 Tenth International Conference on Social Networks Analysis, Management and Security (SNAMS)* (2023), 1–8. <https://api.semanticscholar.org/CorpusID:258309482>
 - [32] Google. 2024. Gemini API. <https://ai.google.dev/gemini-api> Accessed: 2024-06-06.
 - [33] Google AI. 2024. API Overview. <https://ai.google.dev/gemini-api/docs/api-overview> Accessed: 2024-06-06.
 - [34] Jian Gu, Pasquale Salza, and Harald C. Gall. 2022. Assemble Foundation Models for Automatic Code Summarization. *2022 IEEE International Conference on Software Analysis, Evolution and Reengineering (SANER)* (2022), 935–946. <https://api.semanticscholar.org/CorpusID:245986582>
 - [35] Xinying Hou, Yanjie Zhao, Yue Liu, Zhou Yang, Kailong Wang, Li Li, Xiapu Luo, David Lo, John C. Grundy, and Haoyu Wang. 2023. Large Language Models for Software Engineering: A Systematic Literature Review. *ArXiv abs/2308.10620* (2023). <https://api.semanticscholar.org/CorpusID:261048648>
 - [36] Ronald Jabangwe, Henry Edison, and Anh Nguyen-Duc. 2018. Software engineering process models for mobile app development: A systematic literature review. *J. Syst. Softw.* 145 (2018), 98–111. <https://api.semanticscholar.org/CorpusID:52961621>
 - [37] Shuyang Jiang, Yuhao Wang, and Yu Wang. 2023. SelfEvolve: A Code Evolution Framework via Large Language Models. *ArXiv abs/2306.02907* (2023). <https://api.semanticscholar.org/CorpusID:259076266>
 - [38] Kati Kuusinen and Tommi Mikkonen. 2013. Designing User Experience for Mobile Apps: Long-Term Product Owner Perspective. *2013 20th Asia-Pacific Software Engineering Conference (APSEC)* 1 (2013), 535–540. <https://api.semanticscholar.org/CorpusID:18632493>
 - [39] Hugo Laurençon, Léo Tronchon, and Victor Sanh. 2024. Unlocking the conversion of Web Screenshots into HTML Code with the WebSight Dataset. *arXiv:2403.09029* [cs.HC]
 - [40] Valéria Lelli, Arnaud Blouin, and Benoît Baudry. 2015. Classifying and Qualifying GUI Defects. *2015 IEEE 8th International Conference on Software Testing, Verification and Validation (ICST)* (2015), 1–10. <https://api.semanticscholar.org/CorpusID:2288032>
 - [41] Junnan Li, Dongxu Li, Silvio Savarese, and Steven Hoi. 2023. Blip-2: Bootstrapping language-image pre-training with frozen image encoders and large language models. In *International conference on machine learning*. PMLR, 19730–19742.
 - [42] Jia Li, Ge Li, Yongming Li, and Zhi Jin. 2023. Enabling Programming Thinking in Large Language Models Toward Code Generation. *ArXiv abs/2305.06599* (2023). <https://api.semanticscholar.org/CorpusID:263896057>
 - [43] Tsz On Li, Wen yi Zong, Yibo Wang, Haoye Tian, Y. Wang, and S. C. Cheung. 2023. Nuances are the Key: Unlocking ChatGPT to Find Failure-Inducing Tests with Differential Prompting. *2023 38th IEEE/ACM International Conference on Automated Software Engineering (ASE)* (2023), 14–26. <https://api.semanticscholar.org/CorpusID:258298446>
 - [44] Zongjie Li, Chaozheng Wang, Zhibo Liu, Hao Wang, Shuai Wang, and Cuiyun Gao. 2022. CCTEST: Testing and Repairing Code Completion Systems. *2022 IEEE/ACM 45th International Conference on Software Engineering (ICSE)* (2022), 1238–1250. <https://api.semanticscholar.org/CorpusID:251623193>
 - [45] Shuai Lu, Daya Guo, Shuo Ren, Junjie Huang, Alexey Svyatkovskiy, Ambrosio Blanco, Colin B. Clement, Dawn Drain, Daxin Jiang, Duyu Tang, Ge Li, Lidong Zhou, Linjun Shou, Long Zhou, Michele Tufano, Ming Gong, Ming Zhou, Nan Duan, Neel Sundaresan, Shao Kun Deng, Shengyu Fu, and Shujie Liu. 2021. CodeXGLUE: A Machine Learning Benchmark Dataset for Code Understanding and Generation. *ArXiv abs/2102.04664* (2021). <https://api.semanticscholar.org/CorpusID:231855531>
 - [46] Antonio Mastropaolo, Luca Pascarella, and Gabriele Bavota. 2022. Using Deep Learning to Generate Complete Log Statements. *2022 IEEE/ACM 44th International Conference on Software Engineering (ICSE)* (2022), 2279–2290. <https://api.semanticscholar.org/CorpusID:245906103>
 - [47] Antonio Mastropaolo, Simone Scalabrino, Nathan Cooper, David Nader-Palacio, Denys Poshyvanyk, Rocco Oliveto, and Gabriele Bavota. 2021. Studying the Usage of Text-To-Text Transfer Transformer to Support Code-Related Tasks. *2021 IEEE/ACM 43rd International Conference on Software Engineering (ICSE)* (2021), 336–347. <https://api.semanticscholar.org/CorpusID:231786586>
 - [48] Shervin Minaee, Yuri Boykov, Fatih Porikli, Antonio Plaza, Nasser Kehtarnavaz, and Demetri Terzopoulos. 2021. Image segmentation using deep learning: A survey. *IEEE transactions on pattern analysis and machine intelligence* 44, 7 (2021), 3523–3542.
 - [49] K. Moran, C. Bernal-Cárdenas, M. Curcio, R. Bonett, and D. Poshyvanyk. 2018. Machine learning-based prototyping of graphical user interfaces for mobile apps. *IEEE Transactions on Software Engineering* 46, 2 (2018), 196–221.
 - [50] Kevin Moran, Boyang Li, Carlos Bernal-Cárdenas, Dan Jelf, and Denys Poshyvanyk. 2018. Automated Reporting of GUI Design Violations for Mobile Apps. *2018 IEEE/ACM 40th International Conference on Software Engineering (ICSE)* (2018), 165–175. <https://api.semanticscholar.org/CorpusID:3634687>
 - [51] S. Natarajan and C. Csallner. 2018. P2A: A tool for converting pixels to animated mobile application user interfaces. In *Proceedings of the 5th International Conference on Mobile Software Engineering and Systems*. 224–235.
 - [52] T. A. Nguyen and C. Csallner. 2015. Reverse engineering mobile application user interfaces with remaui (t). In *2015 30th IEEE/ACM International Conference on Automated Software Engineering (ASE)*. 248–259.
 - [53] Erik Nijkamp, Bo Pang, Hiroaki Hayashi, Lifu Tu, Haiquan Wang, Yingbo Zhou, Silvio Savarese, and Caiming Xiong. 2022. CodeGen: An Open Large Language Model for Code with Multi-Turn Program Synthesis. In *International Conference on Learning Representations*. <https://api.semanticscholar.org/CorpusID:252668917>
 - [54] OpenAI. [n. d.]. GPT-4 System Card. <https://openai.com/index/gpt-4v-system-card/>. Accessed: 2024-05-30.
 - [55] OpenAI. 2024. Hello GPT-4o. <https://openai.com/index/hello-gpt-4o/> Accessed: 2024-06-06.
 - [56] OpenAI. 2024. Vision Guide. <https://platform.openai.com/docs/guides/vision> Accessed: 2024-06-06.
 - [57] Kishore Papineni, Salim Roukos, Todd Ward, and Wei-Jing Zhu. 2002. Bleu: a Method for Automatic Evaluation of Machine Translation. In *Annual Meeting of the Association for Computational Linguistics*. <https://api.semanticscholar.org/CorpusID:11080756>
 - [58] Victor Le Pochat, Tom van Goethem, Samaneh Tajalizadehkhoob, Maciej Korczyński, and Wouter Joosen. 2018. Tranco: A Research-Oriented Top Sites Ranking Hardened Against Manipulation. *Proceedings 2019 Network and Distributed System Security Symposium*. <https://api.semanticscholar.org/CorpusID:56367624>
 - [59] Alec Radford, Jong Wook Kim, Chris Hallacy, Aditya Ramesh, Gabriel Goh, Sandhini Agarwal, Girish Sastry, Amanda Askell, Pamela Mishkin, Jack Clark, Gretchen Krueger, and Ilya Sutskever. 2021. Learning Transferable Visual Models From Natural Language Supervision. In *International Conference on Machine Learning*. <https://api.semanticscholar.org/CorpusID:231591445>
 - [60] Shuo Ren, Daya Guo, Shuai Lu, Long Zhou, Shujie Liu, Duyu Tang, M. Zhou, Ambrosio Blanco, and Shuai Ma. 2020. CodeBLEU: a Method for Automatic Evaluation of Code Synthesis. *ArXiv abs/2009.10297* (2020). <https://api.semanticscholar.org/CorpusID:221836101>
 - [61] Raj Sanghvi. 2024. Differences Between Web and Mobile App Development. *BitCot* (2024). <https://www.bitcot.com/blog/differences-between-web-and-mobile-app-development/>
 - [62] Chenglei Si, Yanzhe Zhang, Zhengyuan Yang, Ruibo Liu, and Diyi Yang. 2024. Design2Code: How Far Are We From Automating Front-End Engineering? *ArXiv abs/2403.03163* (2024). <https://api.semanticscholar.org/CorpusID:268248801>
 - [63] Ilya Sutskever, Oriol Vinyals, and Quoc V. Le. 2014. Sequence to Sequence Learning with Neural Networks. *ArXiv abs/1409.3215* (2014). <https://api.semanticscholar.org/CorpusID:7961699>
 - [64] Shengbang Tong, Zhuang Liu, Yuexiang Zhai, Yi Ma, Yann LeCun, and Saining Xie. 2024. Eyes Wide Shut? Exploring the Visual Shortcomings of Multimodal LLMs. *ArXiv abs/2401.06209* (2024). <https://api.semanticscholar.org/CorpusID:266976992>
 - [65] Maria Tsimppoukelli, Jacob L Menick, Serkan Cabi, SM Eslami, Oriol Vinyals, and Felix Hill. 2021. Multimodal few-shot learning with frozen language models. *Advances in Neural Information Processing Systems* 34 (2021), 200–212.
 - [66] Typing.com. 2023. What is the Average Typing Speed? <https://www.typing.com/blog/typing-speed/> Accessed: 2023-06-07.
 - [67] Bolin Wei, Ge Li, Xin Xia, Zhiyi Fu, and Zhi Jin. 2019. Code Generation as a Dual Task of Code Summarization. In *Neural Information Processing Systems*. <https://api.semanticscholar.org/CorpusID:202769028>
 - [68] Jason Wei, Xuezhi Wang, Dale Schuurmans, Maarten Bosma, Ed Huai Hsin Chi, F. Xia, Quoc Le, and Denny Zhou. 2022. Chain of Thought Prompting Elicits Reasoning in Large Language Models. *ArXiv abs/2201.11903* (2022). <https://api.semanticscholar.org/CorpusID:246411621>
 - [69] Jason Wei, Xuezhi Wang, Dale Schuurmans, Maarten Bosma, Fei Xia, Ed Chi, Quoc V Le, Denny Zhou, et al. 2022. Chain-of-thought prompting elicits reasoning in large language models. *Advances in neural information processing systems* 35 (2022), 24824–24837.
 - [70] J. Wu, X. Zhang, J. Nichols, and J. P. Bigham. 2021. Screen parsing: Towards reverse engineering of UI models from screenshots. In *The 34th Annual ACM Symposium on User Interface Software and Technology*. 470–483.
 - [71] Y. Xu, L. Bo, X. Sun, B. Li, J. Jiang, and W. Zhou. 2021. image2emmet: Automatic code generation from web user interface image. *Journal of Software: Evolution and Process* 33, 8 (2021), e2369.
 - [72] Zhengyuan Yang, Linjie Li, Kevin Lin, Jianfeng Wang, Chung-Ching Lin, Zicheng Liu, and Lijuan Wang. 2023. The Dawn of LLMs: Preliminary Explorations with GPT-4V(ision). *ArXiv abs/2309.17421* (2023). <https://api.semanticscholar.org/CorpusID:263310951>
 - [73] Pengcheng Yin, Bowen Deng, Edgar Chen, Bogdan Vasilescu, and Graham Neubig. 2018. Learning to Mine Aligned Code and Natural Language Pairs from Stack Overflow. *2018 IEEE/ACM 15th International Conference on Mining Software Repositories (MSR)* (2018), 476–486. <https://api.semanticscholar.org/CorpusID:43922261>

- [74] Shukang Yin, Chaoyou Fu, Sirui Zhao, Ke Li, Xing Sun, Tong Xu, and Enhong Chen. 2023. A Survey on Multimodal Large Language Models. *ArXiv abs/2306.13549* (2023). <https://api.semanticscholar.org/CorpusID:259243718>
- [75] Hao Yu, Bo Shen, Dezhi Ran, Jiaxin Zhang, Qi Zhang, Yu Ma, Guangtai Liang, Ying Li, Tao Xie, and Qianxiang Wang. 2023. CoderEval: A Benchmark of Pragmatic Code Generation with Generative Pre-trained Models. In *International Conference on Software Engineering*. <https://api.semanticscholar.org/CorpusID:256459413>
- [76] Clemens Zeidler, Christof Lutteroth, Wolfgang Stuerzlinger, and Gerald Weber. 2013. Evaluating Direct Manipulation Operations for Constraint-Based Layout. In *IFIP TC13 International Conference on Human-Computer Interaction*. <https://api.semanticscholar.org/CorpusID:8243987>